

Electronic transport in intermediate sized carbon nanotubes

M. Ahlskog, O. Herranen, A. Johansson, J. Leppäniemi, and D. Mtsuko

Department of Physics and Nanoscience Center, University of Jyväskylä, P.O. Box 35 (YFL), FI-40014 Jyväskylä, Finland

(Received 7 December 2008; revised manuscript received 1 February 2009; published 3 April 2009)

We have studied systematically basic transport properties of multiwalled carbon nanotubes in a relatively unexplored diameter range, corresponding to tubes just slightly larger than single- or double-walled tubes to tubes up to 17 nm in diameter. We find in all the smaller tubes a gap in the transport data which increases with decreasing tube diameter. Within the gap region of several tubes, negative differential resistance was observed at small or moderate biases and at bias values that scaled inversely with the tube diameter. For this latter type of behavior of the conductance, we tentatively propose interlayer resonant tunneling as the cause.

DOI: [10.1103/PhysRevB.79.155408](https://doi.org/10.1103/PhysRevB.79.155408)

PACS number(s): 73.63.Fg, 72.80.Rj, 73.40.Gk

Carbon nanotubes exist as single-walled (SWNT) or multiwalled tubes (MWNT), the latter consisting of several concentric SWNTs. Depending on the symmetry of SWNTs, theory indicates both gapless electronic structures and with a band gap. The semiconducting and metallic properties of SWNTs have by now been well confirmed by spectroscopic and transport measurements.^{1,2} Furthermore, these have revealed their capability to conduct with very long mean free paths, i.e., ballistic conduction.

MWNTs should contain both metallic and semiconducting shells, assuming that their growth mechanism does not prefer either type. The band gap for semiconducting tubes has the dependence on diameter (D) as

$$E_g = \frac{\alpha}{D}, \quad (1)$$

where $\alpha \approx 0.7$ eV nm.¹ From this value it follows, that in MWNTs with D clearly larger than 10 nm, the semiconducting behavior of the outer wall is smeared out at room temperature. Transport measurements on MWNTs have usually been performed on tubes with diameters of 10 nm or more, in some cases exceeding 30 nm.³⁻⁹ In most studies the working assumption has been that the outer layer(s) is solely responsible for the low bias transport properties. One motivation for this assumption is the very large anisotropy of conductance in graphite.

There is a clear difference between the transport properties of SWNTs and MWNTs in that such phenomena as ballistic conduction and quantum-dot behavior are mostly absent in the latter, the reason being carrier localization due to structural disorder. MWNTs typically exhibit diffusive transport behavior. The extent of localization can in some cases be very significant (possibly from weak to strong), and some MWNTs are obviously highly defective. Interlayer effects have to date been rather sparsely studied, in particular experimentally.¹⁰⁻¹² It has been concluded that the interlayer transport mechanism is based on tunneling.¹² There are several complications still to tackle before a full understanding of the electronic properties of MWNTs will emerge. For example, it is well known that, as the diameter increases, the deviations of the structure from the ideal become more pronounced. The outer layers of MWNTs with diameters of several tens of nanometer will then be far from a perfect SWNT.

For diameters up to 10–20 nm, the structural features of MWNTs are reasonably close to the ideal picture of concentric SWNTs, as evidenced, for example, by telescopic extension experiments of the inner layers.¹¹

Semiconducting properties in MWNTs have to date been only occasionally observed.^{10,13} The primary reason is perhaps, as already indicated above, that most experiments have used tubes of such large diameters that the small values of E_g does not make a difference. Also, the structural disorder may blur the difference between metallic and semiconducting layers. In SWNTs, with E_g 's close to 1 eV, a strong gap in the current-gate voltage characteristics, in a three terminal conduction measurement, is evident already at room temperature. In small band-gap SWNTs, which are metallic tubes with a gap opening due to the curvature of the wall, the corresponding gap in the gate-dependent conductance is much less pronounced.¹⁴

Thus a general description that covers electronic transport in both single-walled and multiwalled tubes has yet to arise. A systematic experimental study on diameter dependence of MWNTs has to our knowledge been lacking. In this work we present basic transport data on intermediate sized MWNTs ranging in diameter from 3 to 17 nm. In particular, our data covers well the diameter range below 10 nm, which we think complements and bridges previous works on both SWNTs and MWNTs.

MWNTs were obtained from different sources in order to have a wider range of diameters in use.¹⁵⁻¹⁷ Our material should be of a relatively high quality, as judged, for example, by their uniform diameter and straight appearance. Tubes were spin coated onto pieces of Si/SiO₂ substrates from dichloroethane dispersion, after which suitable tubes were located with the AFM. The selected tubes were always straight, smooth, and clean as observed within the resolution limits of the AFM. Au or Pd electrodes (with Ti sticking layer) were fabricated on the MWNTs with electron beam lithography. Figure 1(a) shows an AFM image of a sample where the tube diameter is 6 nm. The total length of the tubes was typically 1–2 μm and always well below 10 μm . The interelectrode spacing varied within 0.5–1.0 μm . The diameters were carefully estimated with AFM by scanning in tapping mode perpendicularly across the tube with a small scan range (< 1 μm). Table I lists the essential experimental data on our samples.

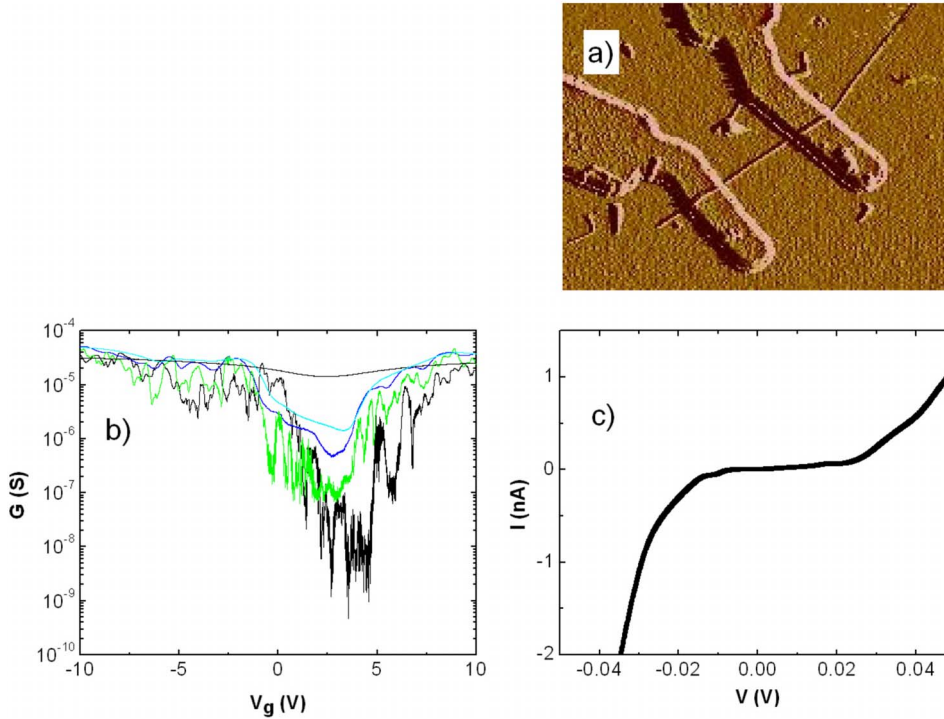


FIG. 1. (Color online) (a) AFM image of a 6-nm-wide contacted tube, sample NT-1 from Table I. (b) Conductance G vs gate voltage V_g at different temperatures (from top to bottom curve: 300, 65, 26, 6, and 4.2 K). (c) Current I vs bias voltage V at $T = 4.2$ K, for the same tube, taken at $V_g = 3.6$ V, where conductance is at its minimum.

The highly doped Si acted as a backgate for applying a gate voltage, with the thickness of the SiO_2 around $0.5 \mu\text{m}$. Conductance measurements were undertaken with both lock-in and dc techniques. Room-temperature measurements were performed either in air or in vacuum. For cooling, usually in a 4 K bath cryostat, the samples were in a helium atmosphere and at the lowest temperature (4.2 K) in vacuum.

Figure 1(b) shows the gate voltage dependent conductance (G vs V_g) of sample NT-1 in Table I at different temperatures. The typical minimum resistance of our tubes at room temperature was in the range 10–50 k Ω , which is relatively close to the minimum value for ballistically conducting SWNTs, $R_q/2 = 6.5$ k Ω ,¹ and implies a small or moderate contact resistance (R_q is the quantum of resistance,

$h/2e^2$). In no obvious way did the room-temperature resistance scale with the length (within the range used here) or with the diameter of the measured tubes (with the exception of sample NT-C, which may simply have a larger contact resistance). The 6 nm diameter tube in the figure has a strong dip in the conductance at intermediate V_g 's, which becomes apparent at low temperatures. Multiwalled tubes with a larger diameter have typically a weaker temperature dependence of resistance. We find the gap in the G vs V_g curves to increase with decreasing tube diameter. At low temperatures, at a few 10 s of Kelvin, reproducible fluctuations in the conductance arise, as mesoscopic transport phenomena^{2,8} are no longer thermally washed out.

The size of the gap can be estimated from the temperature dependence of the G vs V_g characteristics (at zero or small bias). Figure 1(c) shows also low temperature (4.2 K) I - V data for the tube, taken at a gate voltage corresponding to the conductance minimum. As an estimate based on this data, this tube has a gap of 40 meV. This roughly corresponds to the measured temperature dependence since the data of Fig. 1(b) shows the gap of NT-1 being thermally smeared out at 300 K. (Generally, however, the voltage drop across a nanotube is not equivalent to the gap).

In most of our samples, the conductance outside the gap region (in G vs V_g) exhibits a small decrease as well. However, in all cases the temperature dependence at negative V_g shows a saturating zero-bias conductance as $T \rightarrow 0$. This contrasts with the behavior of semiconducting SWNTs where, except for devices with very short tube sections between the electrodes, the zero-bias conductance eventually freezes out upon decreasing temperature.¹⁸

Figure 2 shows an overview of the data from the temperature dependent G vs V_g data of tubes of different diameters. We display minimum zero-bias conductances (G_{\min}) at 4.2 K as a function of D [for example, in Fig. 1(b), G_{\min} is at V_g

TABLE I. Experimental data on the samples used in this work. Listed are source of nanotubes, electrode spacing, diameter, resistance at 300 K, and maximum resistance at 4.2 K (inverse of G_{\min}).

Sample	Source (Ref.)	L_{el} (μm)	D (nm)	R (300 K) (k Ω)	R_{\max} (4 K) (M Ω)
NT-1	15	0.7	6	53.7	2130
NT-7	15	0.72	8	35.6	59.5
NT-9	15	0.8	8	26.9	5.55
NT-2	16	0.69	17	29.6	0.09
NT-4	16	0.91	8.5	42.6	2.77
NT-8	16	0.99	13	33.6	0.19
NT-12	16	0.73	13	36.7	0.14
NT-15	16	0.8	15	34.0	0.14
NT-A	15	0.9	7	50	Not meas.
NT-B	15	1.35	8	20	Not meas.
NT-C	17	0.88	2.8	500	Not meas.

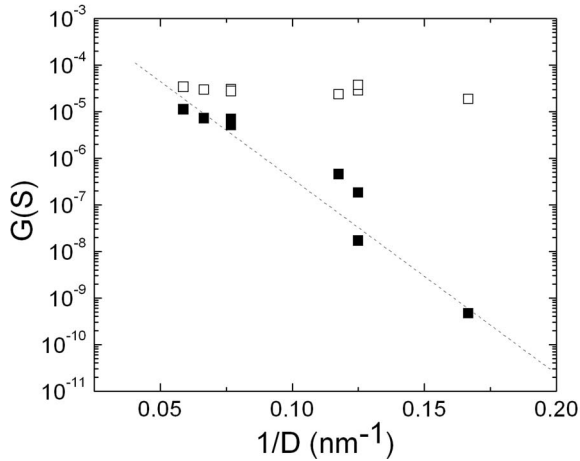


FIG. 2. Minimum measured gate voltage dependent conductance G_{\min} at 4.2 K (■) and the room-temperature values (○) vs inverse diameter (d) of MWNTs. Samples from Table I, excluding the three last ones.

$=3.6$ V; G_{\min} was obtained from the I - V curve at the particular value of V_g]. The room-temperature values of G are also displayed. As the diameter decreases the gap in the G vs V_g data systematically becomes more pronounced. We emphasize here that this trend concerns tubes that clearly are bigger than SWNTs. Among SWNTs we find (also) tubes with no gap.

A closer look at the gap region in a MWNT reveals a complicated behavior as shown in Fig. 3(a), for sample NT-A. We note that as the resistance increases upon the gate voltage entering the gap region, regular Coulomb oscillations are superimposed on the current at low biases [Fig. 3(b)]. The oscillations are visible within the edges of the gap region under some not precisely known conditions. They appear as the resistance becomes $\gg R_q$. In semiconducting SWNT's, these are commonly explained with the emergence

of strong Schottky barriers at the contacts, which forms a single Coulomb island from a tube with low intrinsic charge-carrier scattering.^{19–21} The period of oscillations in this tube is 11 mV. Typically we find Coulomb oscillation periods of 10–30 mV.

In Fig. 3(a), I vs V_g is shown at four different bias voltages. At closer inspection one can note that the current curves cross each other at certain gate voltage intervals. This effect of negative differential resistance (NDR) is also seen by measuring I - V at the same gate voltages in the gap region, as shown in Fig. 3(c). The figure also shows the temperature dependence of this I - V curve. The features disappear as the temperature rises above 20 K.

Generally, the curves are reproducible, if the dip is strong enough, both in the sense that the forward and backward sweeps of the drain-source voltage follow the same curve and that the curves are repeatable over time. However, the occasional case when a weak NDR feature does not reappear in consecutive measurements testifies that the effect is sensitive to minute changes in the local charge environment of the tube. This is understandable in light of the known hysteresis in the G vs V_g characteristics of carbon nanotube devices, which is ascribed to such factors.²²

We observe NDR in some but not all of the MWNTs with diameter well below 10 nm. As was stated above, the effect is observable at certain values of V_g . Figure 4(a)–4(c) shows $dI(V)/dV$ or the differential conductance $G(V)$, taken from measured I - V curves that exhibit NDR, of tubes of different diameter. In the figure zero conductance is indicated with a line so that the regions of NDR are readily observed in the figure.

We will now discuss the main results. One of them is the compiled data shown in Fig. 2 that shows how the dip in the G vs V_g curves at low temperature deepens, in inverse proportion to the diameter. A recent study on transport through graphene strips of different widths found similarly a gap opening when the width was reduced well below 100 nm.²³

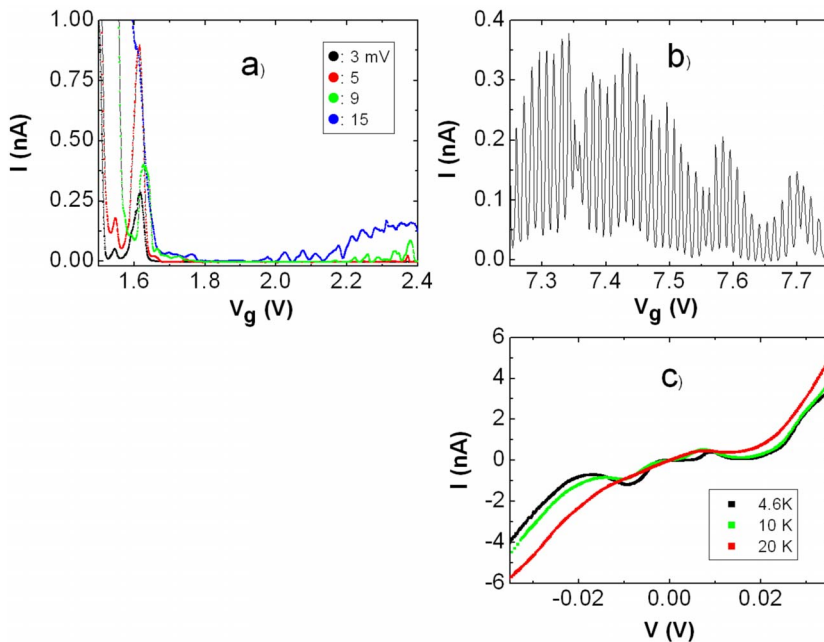


FIG. 3. (Color online) Sample NT-A (a) Current I vs V_g , at bias voltages V from 3 to 15 mV. (b) Coulomb oscillations with $V = 1$ mV, $T = 4.2$ K, in both data sets. (c) Temperature dependence of I - V curves exhibiting NDR. Taken at $V_g = 1.6$ V.

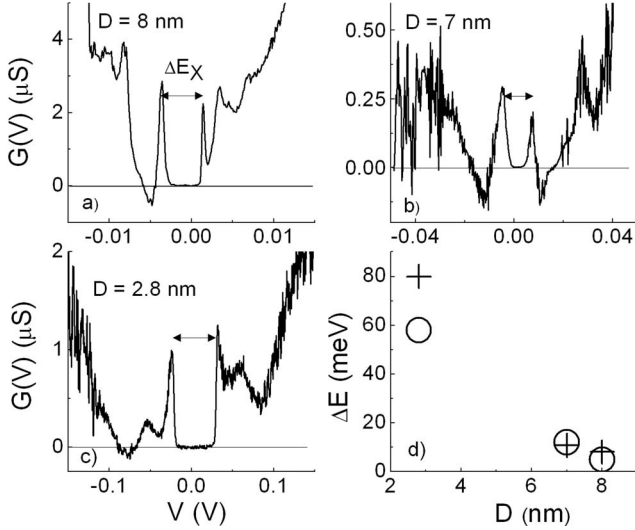


FIG. 4. [(a)–(c)] $G(V)=dI/dV$ for three tubes of different diameters (d) at 4.2 K. Taken at V_g 's within their gap region. Samples are, clockwise from (a) [ignoring (d)]: NT-B, NT-A, and NT-C. The curve in (b) is the derivative of the 4.6 K curve in Fig. 3(c). (d) ΔE , as the measured entity ΔE_X (○) given in (a) and the text, and as the calculated $\Delta E_{g,n}$ (+) from Eq. (3) for the same D values [of the samples in (a)–(c)].

In the case of SWNTs, the gap opening is directly related to the semiconductor-type band structure, as discussed previously. In our results, if the distribution of metallic and semiconducting shells in MWNTs should at all follow their theoretical proportions, then the absence of metallically behaving samples among the $D < 10$ nm tubes is very notable. Another possibility to account for the transport behavior is to relate the gap opening to structural disorder. The disorder creates localized states at the band edges, and if the gate voltage shifts the Fermi level to the corresponding energies, strong localization can be induced. The overall dependence on V_g , T , and V is rather complicated, but we may attempt to model the D dependence in Fig. 2, assuming semiconducting outer shells. The conductance in the gap region may as a first approximation be given as $G \sim \exp[-E_g/k_B T]$. Using Eq. (1) for E_g , and assuming transport dominated by the outer layer, we have

$$\log G \sim \frac{1}{k_B T D} \alpha. \quad (2)$$

From Fig. 2 we obtain $\alpha=0.015$ eV nm (with $T=4.2$ K), which is far too small compared to the α value obtained for SWNTs (0.7 eV nm). Therefore, with semiconducting behavior, a model based on transport through an outer shell solely seems not sufficient, as has been forwarded repeatedly in the case of metallic and diffusive MWNTs.⁴ But, even if the disorder plays a key role, the data shows that the diameter is a determining parameter.

Also, interlayer transport mechanisms will certainly need to be incorporated for a satisfactory model for MWNT transport properties. We think this relates to the other novel aspect in our results, namely, the persistent occurrence of NDR

within the gap region of our samples. NDR arises in many different situations, with the Gunn effect²⁴ and structures with resonant tunneling²⁵ being the most well-known examples. Among the latter, semiconductor heterostructure devices are most prominent, but NDR from this effect has been observed in molecular devices as well.^{26–28} NDR has previously been observed in carbon nanotubes^{19,29–31} but to our knowledge mainly either at high biases²⁹ or in engineered nanotubes.^{30,31} Also, such effects have been estimated theoretically in SWNT devices.³² In our results NDR occurs at low or moderate voltage biases (1–100 mV) and in semiconducting tubes that have not been engineered in any way prior or during fabrication of contacts (otherwise than by the standard fabrication methods described above).

If we assume that the NDR in our case stems from interlayer effects to the conduction, we may look for an explanation from resonant tunneling between adjacent layers. The bias voltage V then aligns energetically the band structures, and maxima in density of states, of adjacent layers in such a manner that resonant conditions arise at certain values of V . This could yield the maxima, and consequent minima, in the observed current.

We next estimate the required bias voltage to shift the energy levels for resonance to occur. We recall that for semiconducting tubes the band gaps are a direct function of the diameter [Eq. (1)]. The diameter between two consecutive layers differs by 2×0.34 nm = 0.68 nm since the interlayer distance in MWNTs is close to that of graphite (0.34 nm). The difference in band gap between two consecutive layers (n and $n+1$) is then

$$\begin{aligned} \Delta E_{g,n} &= E_{g,n} - E_{g,n+1} = \alpha \left[\frac{1}{D_n} - \frac{1}{D_{n+1}} \right] \\ &= \alpha \left[\frac{1}{D_n} - \frac{1}{D_n + 0.68 \text{ nm}} \right]. \end{aligned} \quad (3)$$

In Fig. 4(d), for the diameters of the tubes in Figs. 4(a)–4(c), the calculated $\Delta E_{g,n}$ is shown, along with the measured primary gaps between conductance peaks (ΔE_X), which are indicated explicitly in Figs. 4(a)–4(c). It can be seen from this figure that these values, and in particular their D dependence, correspond roughly with each other. A model based on interlayer resonant tunneling processes may then account for the measured NDR effect in these intermediate sized carbon nanotubes. As we stated above, we observe NDR in some but not all of the tubes with $D < 10$ nm. With our proposed model, it is natural to assume differences in interlayer tunneling with different chiralities of the shells of the MWNT. Therefore, we are confident that the effect is an intrinsic feature of these tubes and that the variation results from the variation in the precise structure of the tubes. A more thorough analysis of NDR as it develops as a function of the gate voltage will take further work.

In summary, we have measured transport properties of carbon nanotubes with diameters intermediate between single-walled or double-walled tubes and the larger ($D > 10$ nm) multiwalled tubes. Below 10 nm diameter, the tubes have a gap in the G vs V_g characteristics in inverse

proportion to the diameter. Moreover, many of these exhibit NDR within the gap region. The NDR occurs at bias voltages also inversely proportional to the diameter. Our results should provide data to an improved understanding of inter-layer transport mechanisms in MWNTs.

This work was funded by the Academy of Finland. A part of the work was done by one of the authors (M.A.) at the Low Temperature Laboratory of the Helsinki University of Technology. We thank S. Iijima, M. Yudasaka, and A. Koshio (NEC Corp., Japan) for supplying us with MWNT material.

-
- ¹ *Carbon Nanotubes*, edited by A. Jorio, M. Dresselhaus, and G. Dresselhaus (Springer, New York, 2008).
- ² J.-C. Charlier, X. Blase, and S. Roche, *Rev. Mod. Phys.* **79**, 677 (2007).
- ³ S. Frank, P. Poncharal, Z. L. Wang, and W. A. de Heer, *Science* **280**, 1744 (1998).
- ⁴ C. Schönenberger, A. Bachtold, C. Strunk, J.-P. Salvetat, and L. Forro, *Appl. Phys. A: Mater. Sci. Process.* **69**, 283 (1999).
- ⁵ R. Tarkiainen, M. Ahlskog, A. Zyuzin, P. Hakonen, and M. Paalanen, *Phys. Rev. B* **69**, 033402 (2004).
- ⁶ B. Bourlon, D. C. Glattli, B. Placais, J. M. Berroir, C. Miko, L. Forro, and A. Bachtold, *Phys. Rev. Lett.* **92**, 026804 (2004).
- ⁷ A. Kanda, K. Tsukagoshi, Y. Aoyagi, and Y. Ootuka, *Phys. Rev. Lett.* **92**, 036801 (2004).
- ⁸ B. Stojetz, C. Miko, L. Forro, and C. Strunk, *Phys. Rev. Lett.* **94**, 186802 (2005).
- ⁹ B. Raquet, R. Avriller, B. Lassagne, S. Nanot, W. Escoffier, J.-M. Broto, and S. Roche, *Phys. Rev. Lett.* **101**, 046803 (2008).
- ¹⁰ P. G. Collins, M. Hersam, M. Arnold, R. Martel, and Ph. Avouris, *Phys. Rev. Lett.* **86**, 3128 (2001).
- ¹¹ J. Cumings and A. Zettl, *Phys. Rev. Lett.* **93**, 086801 (2004).
- ¹² B. Bourlon, C. Miko, L. Forro, D. C. Glattli, and A. Bachtold, *Phys. Rev. Lett.* **93**, 176806 (2004).
- ¹³ M. R. Buitelaar, A. Bachtold, T. Nussbaumer, M. Iqbal, and C. Schönenberger, *Phys. Rev. Lett.* **88**, 156801 (2002).
- ¹⁴ C. Zhou, J. Kong, and H. Dai, *Phys. Rev. Lett.* **84**, 5604 (2000).
- ¹⁵ A. Koshio, M. Yudasaka, and S. Iijima, *Chem. Phys. Lett.* **356**, 595 (2002).
- ¹⁶ Commercial source for carbon nanotubes: MER Corp., USA.
- ¹⁷ Commercial source for carbon nanotubes: Nanocyl, Belgium.
- ¹⁸ A. Javey, J. Guo, Q. Wang, M. Lundstrom, and H. Dai, *Nature (London)* **424**, 654 (2003).
- ¹⁹ J. Park and P. L. McEuen, *Appl. Phys. Lett.* **79**, 1363 (2001).
- ²⁰ P. Jarillo-Herrero, S. Sapmaz, C. Dekker, L. P. Kouwenhoven, and H. S. J. van der Zant, *Nature (London)* **429**, 389 (2004).
- ²¹ A. Makarovski, J. Liu, and G. Finkelstein, *Phys. Rev. Lett.* **99**, 066801 (2007).
- ²² S. Kar, A. Vijayaraghavan, C. Soldano, S. Talapatra, R. Vajtai, O. Nalamasu, and P. M. Ajayan, *Appl. Phys. Lett.* **89**, 132118 (2006).
- ²³ M. Y. Han, B. Özyilmaz, Y. Zhang, and P. Kim, *Phys. Rev. Lett.* **98**, 206805 (2007).
- ²⁴ K. Seeger, *Semiconductor Physics* (Springer, Heidelberg, 1989).
- ²⁵ M. J. Kelly, *Low-Dimensional Semiconductors* (Clarendon, Oxford, 1995).
- ²⁶ Y. Xue, S. Datta, S. Hong, R. Reifenberger, J. I. Henderson, and C. P. Kubiak, *Phys. Rev. B* **59**, R7852 (1999).
- ²⁷ J. Chen, M. A. Reed, A. M. Rawlett, and J. M. Tour, *Science* **286**, 1550 (1999).
- ²⁸ C. Zeng, H. Wang, B. Wang, J. Yang, and J. G. Hou, *Appl. Phys. Lett.* **77**, 3595 (2000).
- ²⁹ E. Pop, D. Mann, J. Cao, Q. Wang, K. Goodson, and H. Dai, *Phys. Rev. Lett.* **95**, 155505 (2005).
- ³⁰ C. Zhou, J. Kong, E. Yenilmez, and H. Dai, *Science* **290**, 1552 (2000).
- ³¹ G. Buchs, P. Ruffieux, P. Gröning, and O. Gröning, *Appl. Phys. Lett.* **93**, 073115 (2008).
- ³² F. Leonard and J. Tersoff, *Phys. Rev. Lett.* **85**, 4767 (2000).